

# Slow Endogenous Fluctuations in Cortical fMRI Signals Correlate with Reduced Performance in a Visual Detection Task and Are Suppressed by Spatial Attention

David W. Bressler, Ariel Rokem\*, and Michael A. Silver

## Abstract

■ Spatial attention improves performance on visual tasks, increases neural responses to attended stimuli, and reduces correlated noise in visual cortical neurons. In addition to being visually responsive, many retinotopic visual cortical areas exhibit very slow (<0.1 Hz) endogenous fluctuations in functional magnetic resonance imaging signals. To test whether these fluctuations degrade stimulus representations, thereby impairing visual detection, we recorded functional magnetic resonance imaging responses while human participants performed a target detection task that required them to allocate spatial attention to either a rotating wedge stimulus or a central fixation point. We then measured the effects of spatial attention on response amplitude at the frequency of wedge rotation and on the amplitude of endogenous fluctuations at nonstimulus frequencies. We found that, in addition to enhancing stimulus-evoked responses,

attending to the wedge also suppressed slow endogenous fluctuations that were unrelated to the visual stimulus in topographically defined areas in early visual cortex, posterior parietal cortex, and lateral occipital cortex, but not in a nonvisual cortical control region. Moreover, attentional enhancement of response amplitude and suppression of endogenous fluctuations were dissociable across cortical areas and across time. Finally, we found that the amplitude of the stimulus-evoked response was not correlated with a perceptual measure of visual target detection. Instead, perceptual performance was accounted for by the amount of suppression of slow endogenous fluctuations. Our results indicate that the amplitude of slow fluctuations of cortical activity is influenced by spatial attention and suggest that these endogenous fluctuations may impair perceptual processing in topographically organized visual cortical areas. ■

## INTRODUCTION

Visual processing and perception are enhanced at attended locations (Carrasco, 2011), and in many visual cortical areas, stimulus-evoked responses of individual neurons are larger when spatial attention is directed to the neuron's receptive field (Maunsell, 2015). In human fMRI studies, the BOLD (blood oxygenation level-dependent) response to a stimulus in visual cortex is greater when attention is directed to the stimulus location (Gandhi, Heeger, & Boynton, 1999).

Spatial attention can also improve visual processing by suppressing brain activity. There is a sustained decrease in BOLD signal in portions of early visual cortex that represent unattended visual field locations (Silver, Ress, & Heeger, 2007; Müller & Kleinschmidt, 2004). Moreover, electrophysiology studies in animal models have shown that spatial attention can decrease variability of stimulus-evoked responses (Mitchell, Sundberg, & Reynolds, 2007) as well as the shared variability (noise correlations) in

populations of neurons (Ruff & Cohen, 2014; Herrero, Gieselmann, Sanayei, & Thiele, 2013; Cohen & Maunsell, 2009; Mitchell, Sundberg, & Reynolds, 2009).

In a previous study, we used a periodic visual stimulus, a spatial attention task, and fMRI to study the effects of attention on the reliability of stimulus-evoked responses in many topographically organized areas in early visual, ventral occipital, lateral occipital, and posterior parietal cortex (Bressler & Silver, 2010). Participants performed a target detection task that required them to maintain spatial attention either within a rotating wedge stimulus or at a central fixation point. We found that, relative to attending to the fixation point, continuously directing attention to the rotating wedge improves the reliability of fMRI responses evoked by the wedge (Bressler & Silver, 2010).

In this study, we used Fourier decomposition to simultaneously and independently estimate both stimulus-evoked and endogenous fMRI signals in the same time series. Because the rotating wedge stimulus generated a periodic response in voxels in cortical areas containing a topographic map of the visual field, we could distinguish this evoked response from ongoing endogenous fluctuations in the frequency domain (Engel et al.,

---

University of California, Berkeley

\*A. R. is currently at the University of Washington eScience Institute.

1994). We found that the improved reliability of fMRI responses to an attended periodic visual stimulus (Bressler & Silver, 2010) is due to both an enhancement of the stimulus-evoked response and a reduction in the amplitude of endogenous slow fluctuations that are unrelated to the stimulus. In addition, the relative contributions of response enhancement and suppression of endogenous fluctuations to improved response reliability varied across topographically organized cortical areas, and the amplitudes of enhancement and suppression were not correlated across 5-min fMRI runs.

We also correlated performance on the visual detection task with the amplitude of both stimulus-evoked responses and endogenous fluctuations. In multiple cortical areas, larger fMRI responses predict detection of a threshold-level stimulus (Imamoglu, Heinzle, Imfeld, & Haynes, 2014; Ress, Backus, & Heeger, 2000). However, attentional suppression of endogenous fluctuations could also improve the brain's representation of the attended stimulus, thereby facilitating perception of the attended stimulus. Perceptual performance is affected by intrinsic neural activity immediately before stimulus presentation (Busch, Dubois, & VanRullen, 2009; Mathewson, Gratton, Fabiani, Beck, & Ro, 2009; Supèr, van der Togt, Spekreijse, & Lamme, 2003), including very slow (<0.1 Hz) fluctuations in activity (Monto, Palva, Voipio, & Palva, 2008). In addition, ongoing fMRI signals before initiation of visual perceptual tasks predict behavior (Coste & Kleinschmidt, 2016; Wohlschläger et al., 2016; Hesselmann, Kell, & Kleinschmidt, 2008; Weissman, Roberts, Visscher, & Woldorff, 2006).

We found that the magnitude of slow endogenous fluctuations predicted participants' performance on a visual target detection task in all 11 of the occipital and parietal cortical areas that we studied. Specifically, target detection performance was greatest when the strength of suppression of slow endogenous fluctuations was largest. Surprisingly, we did not find a relationship between the amplitude of the stimulus-evoked response and behavioral performance in any cortical area. These results suggest that endogenous fluctuations in neural activity are modulated by spatial attention and that successful suppression of this endogenous activity facilitates visual perception.

## METHODS

Visual stimuli, task design, fMRI data collection and preprocessing, and definition of topographically organized cortical areas have been described (Bressler & Silver, 2010) and will only be summarized here.

### fMRI Data Acquisition and Preprocessing

fMRI experiments were conducted for five participants with a 4T Varian INOVA MR scanner and for the other five participants with a 3T Siemens MAGNETOM Trio MR

scanner. In the 4T scanner, a transmit/receive surface radiofrequency coil was used to maximize the contrast-to-noise ratio in occipital cortex, and in the 3T scanner, a 12-channel receive-only head coil was used. Functional echo-planar images were acquired using a gradient-echo EPI sequence. The field of view was 180 × 180 (4T) or 200 × 200 mm (3T), and the matrix size was 64 × 64 (4T) or 96 × 96 (3T), resulting in an in-plane voxel resolution of 2.81 (4T) or 2.08 mm (3T). The repetition time was 1.067 (4T) or 2.133 sec (3T), and the echo time was 28 (4T) or 26 msec (3T). Twenty (4T) or 22 (3T) slices were prescribed with an interslice gap of 0.3 mm and a slice thickness of 3 mm (4T) or 2 mm (3T).

The duration of each run was 281.6 sec, and the first 8.53 sec of the fMRI time series were discarded. Head movements were corrected offline using a 3-D image registration algorithm (MCFLIRT; Jenkinson, Bannister, Brady, & Smith, 2002). For each voxel and fMRI run, the mean fMRI signal across all time points in the run (DC component) was subtracted from each time point in the motion-corrected time series. As we were interested in studying a wide range of temporal frequencies, no additional preprocessing steps (such as transformation to Fisher Z scores, conversion to percent signal change, high-pass filtering, or temporal detrending) were applied to the data.

## Experimental Design and Statistical Analysis

### Participants

In addition to the eight participants described in Bressler and Silver (2010), two additional participants completed this study. All 10 participants (7 female, 3 male) completed one session to acquire high-resolution whole-brain anatomical MR images and one fMRI scanning session. Experiments were undertaken with the understanding and written consent of each participant, and all experimental procedures were approved by the Committee for the Protection of Human Subjects at the University of California, Berkeley.

### Visual Stimuli and Task

A checkerboard wedge stimulus rotating about a central fixation point (Serenio et al., 1995; Engel et al., 1994) was continuously presented during acquisition of each fMRI time series (Figure 1).

The wedge subtended 45° and extended from 0.5° (inner radius) to 10.9° (outer radius) of visual angle. Each check within the wedge reversed contrast at a rate of 7.5 Hz, and the stimulus contrast was 100%. The wedge was presented for 2.13 sec in each location, and the subsequent wedge location was displaced 22.5° in a clockwise direction. Therefore, there were a total of 16 wedge positions, and each position overlapped 50% with the neighboring positions. The wedge completed a

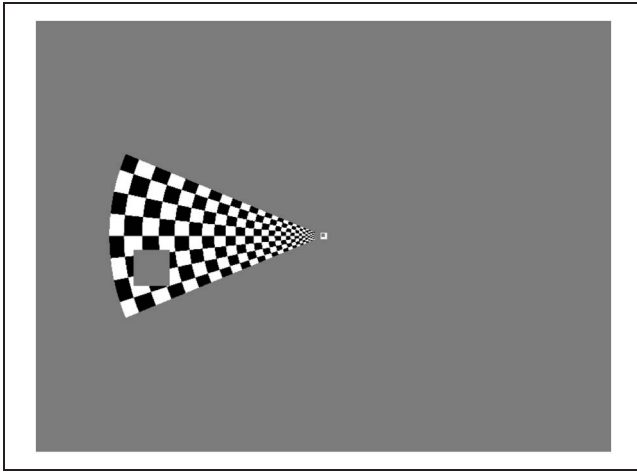


**Figure 1.** Stimulus and tasks. Participants viewed a wedge-shaped stimulus that rotated around the central fixation point while continuously maintaining fixation, and they pressed a button whenever they detected a contrast decrement target. In the attention-to-wedge condition, participants detected targets presented at random locations within the wedge, and in the attention-to-fixation condition, participants detected targets within the fixation point.

full rotation once every 34.13 sec. Participants were instructed to continuously maintain fixation on a central fixation point ( $0.25^\circ$  of visual angle) throughout each scan.

In the attention-to-wedge task, participants were instructed to maintain fixation on the central point and to press a button whenever they detected a brief (0.27 sec) presentation of a square region of zero contrast within the wedge (Figure 1). There was a 50% probability of target presentation at each wedge position, and the target could appear anywhere within the wedge stimulus at unpredictable times. Uncertainty regarding the time and location of target presentation encouraged participants to continuously allocate their attention over the entire wedge. In addition, to avoid the possibility that differences in difficulty of target detection as a function of eccentricity could affect the allocation of spatial attention over the wedge, the target sizes in three eccentricity bands ( $0.5^\circ$ – $4.0^\circ$ ,  $4.0^\circ$ – $7.4^\circ$ , and  $7.4^\circ$ – $10.9^\circ$  of visual angle) were adjusted for each participant to equate the percentage of targets correctly detected in each of these bands. The boundaries between these eccentricity bands were not visible to the participants.

In the attention-to-fixation task, participants were instructed to maintain fixation on the central square and to press a button when they detected a square region of zero contrast within the fixation square. The targets in the attention-to-fixation and attention-to-wedge tasks had identical durations, contrasts, and probabilities of presentation. To equate sensory stimulation in the two tasks, the square zero-contrast regions were presented in both the fixation point and the wedge for both attention conditions (although the temporal sequences of presentation within the fixation point and the wedge were

independent and were based on a 50% probability of presentation for each wedge position). The attention-to-wedge and attention-to-fixation runs always occurred in pairs, with one member of the pair immediately following the other, and any changes to the target sizes were applied to both runs in the pair. Thus, the only difference between the two conditions was that the participants responded to wedge targets in the attention-to-wedge task and to fixation targets in the attention-to-fixation task.

Eye movements were not recorded during the fMRI experiments. However, all participants were highly trained in maintaining fixation through participation in numerous prior psychophysical experiments. Significant deviations from fixation would have reduced our ability to retinotopically define cortical areas, but we defined many areas in each participant in a single scanning session (exact numbers of defined areas per participant are presented below).

Before fMRI data collection, each participant practiced the two target detection tasks for a total of 4 hr in a behavioral testing room, allowing behavioral performance to reach asymptotic levels. In addition, behavioral data from the practice sessions were used to determine the target sizes for each participant that resulted in equivalent performance of the two tasks in the fMRI experiment. During behavioral practice sessions, the size of the fixation target was adjusted to insure that the task difficulty (percentage of fixation targets correctly detected) was equal to that of each of the three eccentricity bands in the attention-to-wedge task. Similar to the eight participants described in Bressler and Silver (2010), there was no significant difference in performance between the attention-to-wedge and attention-to-fixation tasks for either of the additional two participants reported in this study (Participant 9:  $p = .09$ ,  $n = 5$  pairs of runs; Participant 10:  $p = .37$ ,  $n = 6$  pairs of runs; two-tailed  $t$  tests; see Table 1).

#### *Definition of Topographic Cortical Areas and ROIs*

The boundaries of visual cortical areas V1, V2, V3, V3A/B, V4, LO1, LO2, and VO1 and posterior parietal areas IPS0, IPS1, and IPS2 were defined using well-established phase-encoded retinotopic mapping methods (Silver, Ress, & Heeger, 2005; Sereno et al., 1995; Engel et al., 1994).

**Table 1.** Behavioral Performance

<i>Participant No.</i>	<i>Wedge</i>	<i>Fixation</i>	<i>Near</i>	<i>Middle</i>	<i>Far</i>
9	76	64	74	75	81
10	71	63	67	69	77

Values are percentage of targets correctly detected for all trials of the attention-to-wedge task, the attention-to-fixation task, and for each of the three eccentricity bands in the attention-to-wedge task for the two participants not included in Bressler and Silver (2010).

Each participant completed between five and seven attention-to-wedge runs and an equal number of attention-to-fixation runs; the order of runs was interleaved for the two attention conditions. The time series from each voxel were converted to units of percent signal change and averaged across all runs (including both attention-to-wedge and attention-to-fixation). Note that we convert to percent signal change and average across runs only for the purpose of defining the boundaries of topographically organized areas; in our main time-series analysis (see below), there was no conversion to percent signal change.

The duration of the stimulus cycle was 34.13 sec, resulting in a modulation of fMRI signals in visually responsive voxels of  $1/34.13 \text{ sec} = 0.0293 \text{ Hz}$ . Any voxels that responded to the visual stimulus in a spatially specific manner therefore exhibited modulations of activity at this stimulus frequency. We computed the discrete Fourier transform for each time series from each voxel, and response phases at the stimulus frequency (relative to the cycle of the rotating wedge) were spatially transformed and overlaid on computationally flattened cortical patches. The phase of the Fourier-transformed time series at the frequency band containing the stimulus frequency corresponds to the angular component (in polar coordinates) of the visual field location that is represented by a given voxel. The spatial distribution of these response phases on the cortical surface was then used to define the locations and boundaries of topographically organized cortical areas.

Using these procedures, the boundaries of V1, V2, V3, V4, IPS1, and IPS2 were successfully defined in both hemispheres of all participants (total of 20 hemispheres). Of the 20 hemispheres in our sample, V3A/B, IPS0, and LO1 (Larsson & Heeger, 2006) were defined in 19 of these, LO2 (Larsson & Heeger, 2006) and VO1 (Brewer, Liu, Wade, & Wandell, 2005) were defined in 18 hemispheres, and each topographic area was defined in at least one hemisphere for each participant. The locations and boundaries of topographically organized areas in an example hemisphere from a participant not reported in Bressler and Silver (2010) is shown in Figure 2.

In addition to these topographic areas, we also defined a bilateral ROI centered in the posterior cingulate cortex (PCC)/precuneus (Talairach coordinates  $[-2, -51, 27]$ ,  $[2, -51, 27]$ ; Greicius, Krasnow, Reiss, & Menon, 2003). For each participant, the PCC/precuneus ROI was expanded isotropically from the Talairach-defined center within the cortical gray matter (Wandell, Chial, & Backus, 2000) until its volume was equal to the average volume of the defined topographic cortical areas for that participant.

### Time-series Analysis

We applied Fourier decomposition to the time series for each run to compute amplitude at the stimulus frequency and nonstimulus frequencies. The strength of

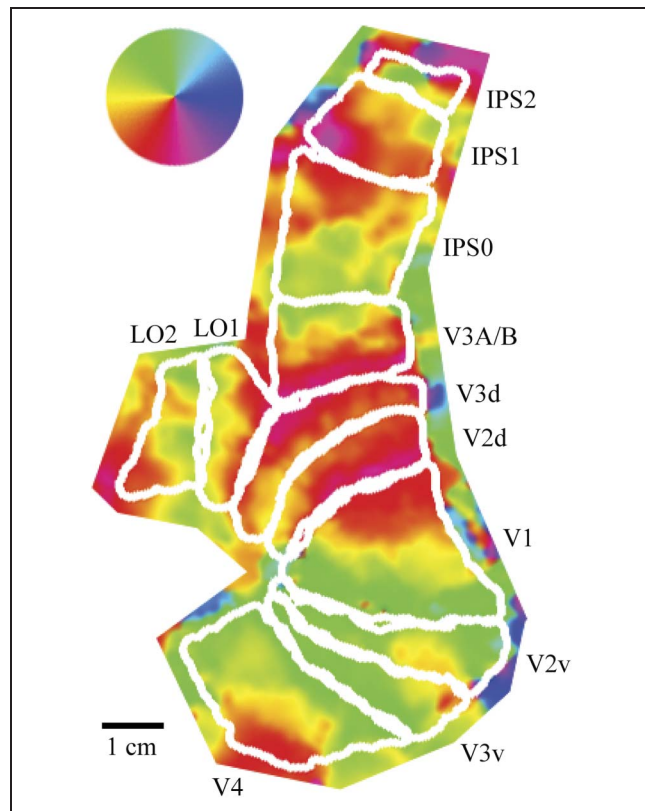


**Figure 2.** Locations and boundaries of topographically organized areas in occipital and parietal cortex. The color wheel indicates the relationship between response phase at the frequency of wedge rotation and the angular component of visual field location. In this right hemisphere example, each area represents the contralateral left visual field.

fluctuation at the stimulus frequency was defined as the amplitude at the frequency band centered on 0.0293 Hz, corresponding to the rate of wedge rotation. We defined the strength of fluctuation at nonstimulus frequencies as the average of amplitudes of frequency components with ranges of 0.0073–0.0220 Hz, 0.0366–0.0513 Hz, 0.0659–0.0806 Hz, and 0.0952–0.0989 Hz (i.e., all frequency components below 0.1 Hz, not including 0 Hz (DC), the stimulus frequency, harmonics of the stimulus frequency, and frequency bands immediately adjacent to these components).

For each voxel, attentional modulation of the amplitudes at stimulus and nonstimulus frequencies was expressed as a contrast index:  $(w - f)/(w + f)$ , where  $w$  is attention-to-wedge and  $f$  is attention-to-fixation. This contrast index is similar to the percent change relative to the attention-to-fixation baseline, but unlike percent change values, contrast indices are symmetric for increases and decreases. Contrast indices were computed for every pair of attention-to-wedge and attention-to-fixation runs, generating unbiased estimates of attentional modulation for every voxel. These contrast index values were averaged across all voxels within each cortical area to obtain a total of 60 attentional modulation values

for the group of 10 participants. For each cortical area, the mean of these 60 contrast index values was compared with a value of zero (indicating no effect of spatial attention) with a two-tailed  $t$  test. All statistical tests that were applied to each of the 12 cortical areas were corrected for multiple comparisons using the false discovery rate (FDR) method (Genovese, Lazar, & Nichols, 2002).

In addition, we estimated the relationship between amplitude at the stimulus frequency and that of nonstimulus frequencies across attention-to-wedge runs. Each 5-min run generated an amplitude value at the stimulus frequency and at nonstimulus frequencies in each voxel, and the correlation of these two amplitudes was computed across runs. These correlation coefficients were then converted to normally distributed  $z$  scores by Fisher transformation and then averaged across all voxels within a given cortical area for each participant. For each area, we assessed whether the mean correlation coefficient across the 10 participants was significantly different from zero using a two-tailed  $t$  test.

We also conducted this correlation analysis across runs using a normalized estimate of stimulus-evoked activity. This normalization was applied to minimize the contribution of endogenous activity to the estimate of stimulus-evoked responses. Endogenous fluctuations occurred at all temporal frequencies we studied, so the amplitude at the stimulus frequency includes both stimulus-evoked activity and endogenous activity. We therefore subtracted the mean of the amplitude at nonstimulus frequency bands immediately adjacent to the stimulus frequency (0.0256 and 0.0330 Hz, providing an estimate of the amount of activity that is in the stimulus frequency band but unrelated to the stimulus) from the amplitude at the

stimulus frequency band (0.0293 Hz) for each voxel. This normalized stimulus frequency amplitude was then correlated with nonstimulus frequency amplitudes across runs as described above.

This normalization procedure was not applied to the calculation of the contrast index values described above ( $[\text{wedge} - \text{fix}]/[\text{wedge} + \text{fix}]$ ; see Figures 3–5). We found that subtracting the mean of the amplitude at nonstimulus frequency bands immediately adjacent to the stimulus frequency from the amplitude at the stimulus frequency band sometimes generated very small difference values, resulting in small values of the denominator of the contrast index and variable and unstable contrast index values. The decision to not apply normalization to contrast index values means that some portion of the amplitude at the stimulus frequency is due to endogenous fluctuations in that frequency band. However, this would only reduce differences between stimulus and nonstimulus frequencies with respect to attentional modulation, and our results clearly demonstrate opposing effects of spatial attention on amplitudes at stimulus and nonstimulus frequencies in the majority of studied topographically organized areas (Figure 3).

### Correlation with Perceptual Performance

For each attention-to-wedge run, behavioral performance was correlated with amplitude at both stimulus and nonstimulus frequencies. Although target size was occasionally adjusted during the fMRI session to maintain equivalent difficulty in the attention-to-fixation and attention-to-wedge tasks, 9 of 10 participants had at least five attention-to-wedge runs with the same target size distribution (with the remaining participant having four

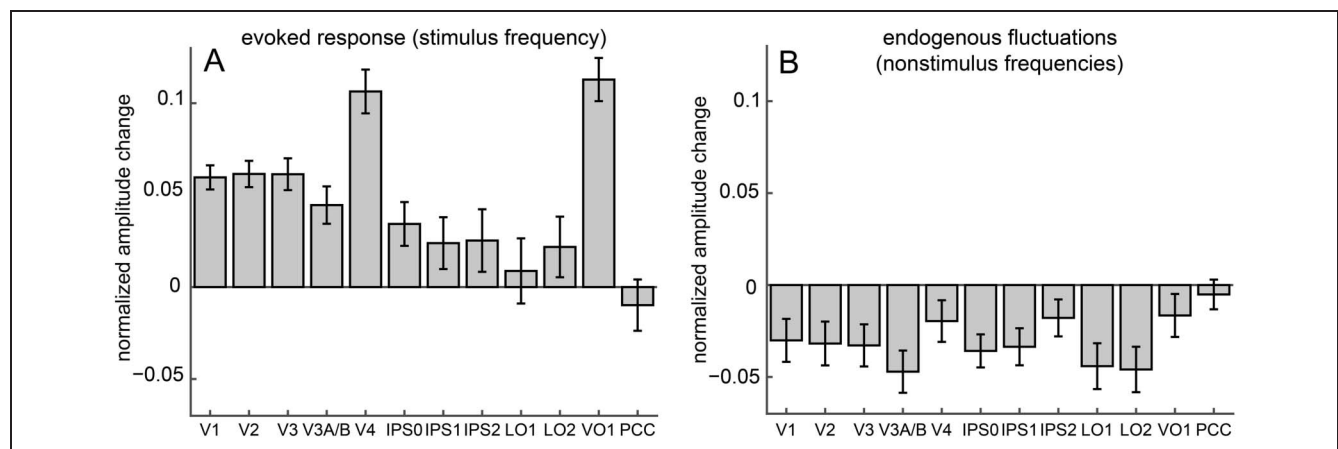


**Figure 3.** Attentional modulation of amplitude of the evoked response and fluctuations at nonstimulus frequencies. Effects of attention were quantified as a contrast index of fMRI signal amplitudes for the two attention conditions:  $(\text{wedge} - \text{fixation})/(\text{wedge} + \text{fixation})$ . (A) Attending to the rotating wedge significantly increased the amplitude of the visual response (stimulus frequency, 0.0293 Hz) in early and ventral visual cortical areas, but not in IPS1, IPS2, LO1, or LO2. (B) In contrast, attending to the wedge decreased the strength of endogenous nonstimulus fluctuations (0.0073–0.1 Hz, excluding the stimulus frequency and its harmonics) in every measured topographically organized area except IPS2, V4, and VO1. These attention effects were not observed in a PCC control region. Error bars represent SEMs across pairs of attention-to-wedge and attention-to-fixation runs.

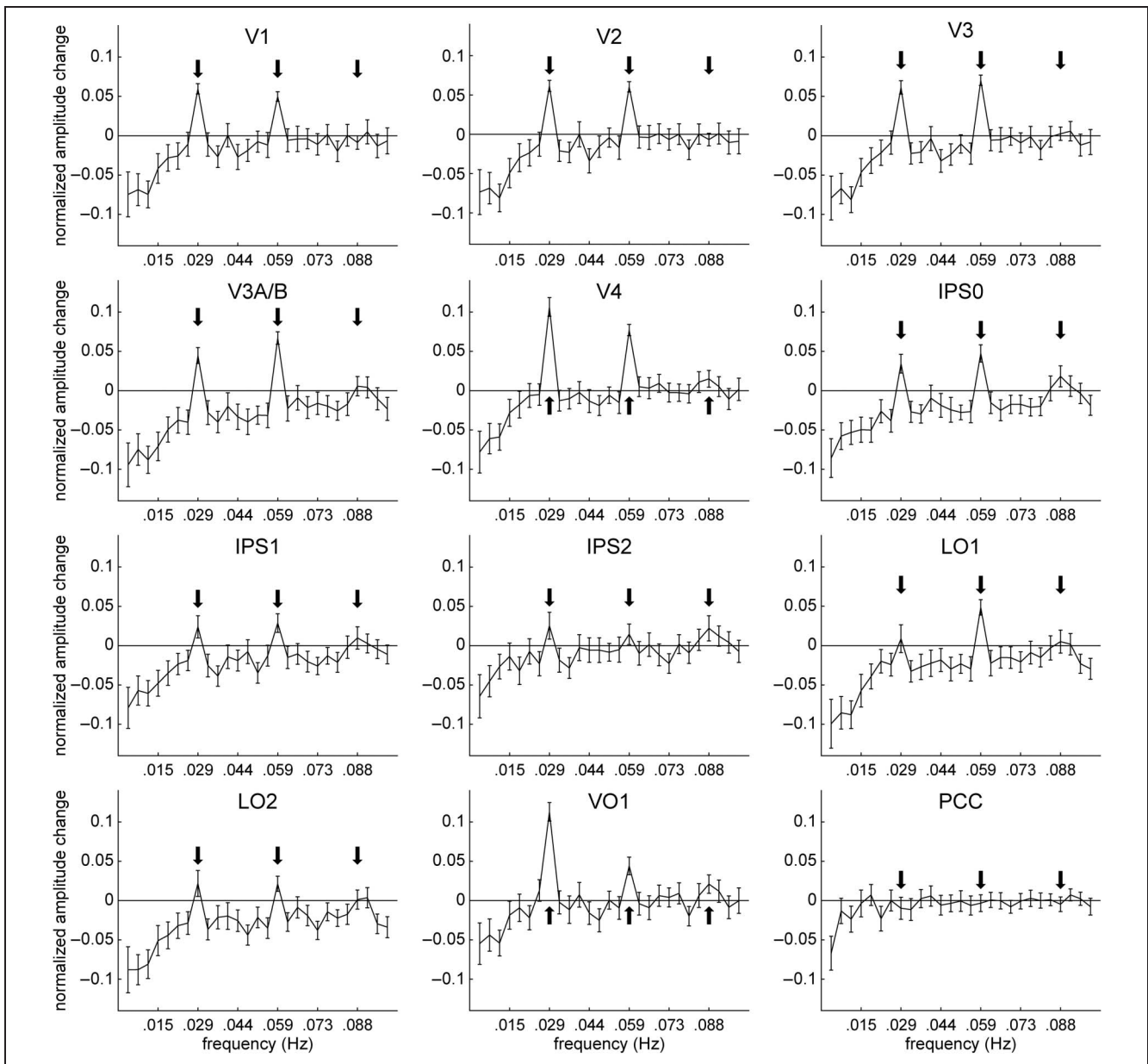


**Figure 4.** Attentional modulation of amplitude of fluctuations across the frequency spectrum. As in Figure 3, effects of attention were quantified as a contrast index of fMRI signal amplitudes for the two attention conditions: (wedge – fixation)/(wedge + fixation). In all topographically organized cortical areas, attending to the wedge stimulus caused suppression of nonstimulus frequency fluctuations that was greatest for the lowest frequencies (approximately less than 0.03 Hz), whereas only a subset of areas showed a significant reduction in higher nonstimulus frequencies. Stimulus frequency (0.029 Hz) and associated harmonics (0.059 and 0.088 Hz) are indicated with arrows. Error bars represent *SEMs* across pairs of attention-to-wedge and attention-to-fixation runs.

attention-to-wedge runs with the same target size distribution). Only sets of runs for which target size distribution did not change were included in the correlation analysis, and this required excluding one run from the data for four participants.

For each participant, we tested whether behavioral performance across attention-to-wedge runs was significantly different from a normal distribution using Kolmogorov–Smirnov tests, and we found that no participant showed significant deviations from normality (all *ps* > .59).

There was also no significant deviation from normality for the distribution of behavioral performance for data pooled across all participant (*p* = .97). Correlation coefficients were converted to normally distributed *z* scores by Fisher transformation and were averaged across all voxels within a given cortical area for each participant. The mean of the *z* scores of the correlation coefficients across the 10 participants was then compared with a value of zero for each cortical area using a two-tailed *t* test.

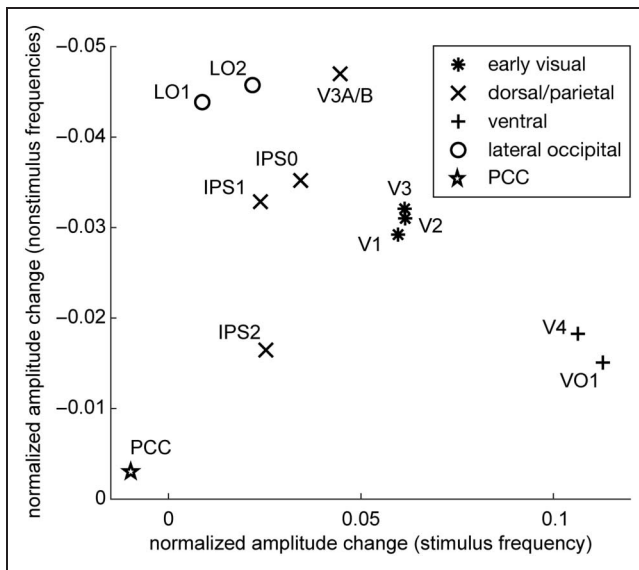


**Figure 5.** Correlation between attentional modulation of amplitude of stimulus and nonstimulus frequencies across topographic areas. Ventral visual (+) areas showed the strongest enhancement of visual responses but the weakest suppression at nonstimulus frequencies, lateral occipital (o) and posterior parietal (X) areas generally showed the opposite pattern of results, and early visual cortical areas (\*) exhibited moderate levels of both enhancement of the visual response and suppression at nonstimulus frequencies.

### Availability of Data and Analysis Code

All the data presented here and associated analysis code are available at <https://osf.io/vznur/>.

## RESULTS

Participants maintained central fixation while viewing a wedge-shaped visual stimulus that rotated around the screen once every 34.13 sec (Figure 1). On separate runs, attention was either maintained at the central fixation point or directed toward the rotating wedge stimulus. During attention-to-fixation runs, participants detected targets that were presented within the fixation point, and in the attention-to-wedge runs, they detected targets that were presented at random locations within the rotating wedge. Participants pressed a button whenever they detected a low-contrast target in the attended region. The difficulty of the task was controlled by adjusting target size for each participant so that they detected approximately 70% of the targets in each attention condition. fMRI responses were recorded from topographically organized cortical areas V1, V2, V3, V3A/B, V4, IPS0, IPS1, IPS2, LO1, LO2, and VO1 as well as a control region in PCC that does not contain a topographic map of the visual field.

### Effects of Spatial Attention on Strength of Fluctuations in fMRI Signals at Stimulus and Nonstimulus Frequencies

The rotating wedge evoked periodic modulation of activity in any brain location that exhibited a spatially specific

response to the stimulus, and the frequency of this modulation was equal to the frequency of wedge rotation (0.0293 Hz). A Fourier transform was computed for each voxel's time series to quantify the amplitude of the evoked response at the stimulus frequency (0.0293 Hz) and at nonstimulus frequencies between 0.0037 and 0.1 Hz. We measured attentional modulation of both of these quantities and found that, relative to attending to fixation, attending to the wedge significantly increased the amplitude of the stimulus-evoked response in cortical areas V1 ( $t = 9.10$ ,  $p = 4.6 \times 10^{-12}$ ), V2 ( $t = 8.59$ ,  $p = 1.7 \times 10^{-11}$ ), V3 ( $t = 7.10$ ,  $p = 4.5 \times 10^{-9}$ ), V3A/B ( $t = 4.39$ ,  $p = 9.5 \times 10^{-5}$ ), V4 ( $t = 8.94$ ,  $p = 5.9 \times 10^{-12}$ ), IPS0 ( $t = 2.88$ ,  $p = 9.4 \times 10^{-3}$ ), and VO1 ( $t = 9.61$ ,  $p = 1.3 \times 10^{-12}$ ), but not in posterior parietal (IPS1:  $t = 1.70$ ,  $p = .14$ ; IPS2:  $t = 1.49$ ,  $p = .19$ ) or lateral occipital (LO1:  $t = 0.49$ ,  $p = .62$ ; LO2:  $t = 1.32$ ,  $p = .23$ ) cortex (Figure 3A; two-tailed  $t$  tests, FDR-corrected,  $df = 59$ ).

Attending to the wedge also significantly decreased the amplitude of slow endogenous fluctuations at nonstimulus frequencies in all topographically organized cortical areas that we tested (V1:  $t = -2.57$ ,  $p = .019$ ; V2:  $t = -2.67$ ,  $p = .017$ ; V3:  $t = -2.87$ ,  $p = .012$ ; V3A/B:  $t = -4.11$ ,  $p = 1.1 \times 10^{-3}$ ; IPS0:  $t = -3.98$ ,  $p = 1.1 \times 10^{-3}$ ; IPS1:  $t = -3.33$ ,  $p = 3.6 \times 10^{-3}$ ; LO1:  $t = -3.54$ ,  $p = 2.4 \times 10^{-3}$ ; LO2:  $t = -3.71$ ,  $p = 1.8 \times 10^{-3}$ ), except V4, IPS2, and VO1 (V4:  $t = -1.73$ ,  $p = .11$ ; IPS2:  $t = -1.78$ ,  $p = .11$ ; VO1:  $t = -1.42$ ,  $p = .18$ ; Figure 3B; two-tailed  $t$  tests, FDR-corrected,  $df = 59$ ).

Examination of power spectra of attentional modulation in individual cortical areas (Figure 4) indicates that attentional suppression was strongest for the lowest frequencies (approximately  $<0.03$  Hz), although this suppression extended to higher frequencies for some cortical areas (e.g., V3A/B, IPS0, LO1, and LO2).

### Relative Contributions of Attentional Enhancement and Suppression to Improved Response Reliability Vary across Topographic Cortical Areas and across Time

We previously showed that directing attention to the rotating wedge increased the reliability of the fMRI response to the wedge in many topographically organized areas in occipital and parietal cortex (Bressler & Silver, 2010). This improved response reliability could be due to increased amplitude of the stimulus-evoked response and/or suppression of endogenous activity unrelated to the representation of the stimulus. To determine the relative contributions of attentional enhancement and suppression to improved response reliability, we correlated the amount of attentional enhancement at the stimulus frequency to the amount of attentional suppression at nonstimulus frequencies across topographic cortical areas. This analysis revealed that lateral occipital and posterior parietal areas generally showed the strongest suppression and weakest enhancement by spatial attention,

ventral visual areas had the strongest enhancement and weakest suppression, and early visual areas exhibited intermediate levels of both enhancement and suppression (Figure 5). In addition, across cortical areas, there is an inverse relationship between the amount of signal enhancement and suppression of endogenous frequencies by spatial attention ( $r = -.65$ ;  $p = .029$ ; Figure 5).

Given that attending to the wedge generally increased the amplitude at the stimulus frequency but decreased the amplitude at nonstimulus frequencies, we also determined whether periods of high stimulus-evoked responses were associated with lower amplitudes of nonstimulus frequencies within a given area across runs. For each voxel, we correlated the amplitude of the evoked response at the stimulus frequency with the amplitude of endogenous fluctuations at nonstimulus frequencies across the 5-min attention-to-wedge runs. These correlation coefficients were significantly greater than zero in all studied topographic areas (V1:  $t = 8.56$ ,  $p = 6.2 \times 10^{-5}$ ; V2:  $t = 9.56$ ,  $p = 6.2 \times 10^{-5}$ ; V3:  $t = 8.36$ ,  $p = 6.2 \times 10^{-5}$ ; V3A/B:  $t = 4.42$ ,  $p = 1.8 \times 10^{-3}$ ; V4:  $t = 4.30$ ,  $p = 2.0 \times 10^{-3}$ ; IPS0:  $t = 4.47$ ,  $p = 1.8 \times 10^{-3}$ ; IPS1:  $t = 7.51$ ,  $p = 8.8 \times 10^{-5}$ ; IPS2:  $t = 5.88$ ,  $p = 4.0 \times 10^{-4}$ ; LO1:  $t = 7.78$ ,  $p = 8.3 \times 10^{-5}$ ; LO2:  $t = 7.01$ ,  $p = 1.3 \times 10^{-4}$ ; VO1:  $t = 4.89$ ,  $p = 1.1 \times 10^{-3}$ ; two-tailed  $t$  tests, FDR-corrected,  $df = 9$ ). However, some of this large positive correlation between amplitudes at stimulus and nonstimulus frequencies across runs is due to the fact that endogenous fluctuations of fMRI signal occur simultaneously at many frequencies (Zarahn, Aguirre, & D'Esposito, 1997), including the stimulus frequency in our data. That is, amplitude at the stimulus frequency represents a combination of stimulus-evoked activity and endogenous fluctuations that are in the same frequency band as the wedge rotation. In addition, very slow fluctuations or drift in overall fMRI power across multiple 5-min runs will lead to positive correlations of amplitude in stimulus and nonstimulus frequency bands.

Thus, to more directly test for correlations between enhancement of response amplitude and suppression of endogenous frequencies across runs, we subtracted the mean of the amplitude in nonstimulus frequency bands on either side of the stimulus frequency from the amplitude at the stimulus frequency on each run. This generated a normalized amplitude at the stimulus frequency that more accurately reflects the magnitude of the stimulus-evoked response while minimizing contribution from endogenous fluctuations. We then computed correlation coefficients between this normalized amplitude at the stimulus frequency and the mean amplitudes of the nonstimulus frequencies across runs. None of the topographic cortical areas exhibited a significant correlation across runs (V1:  $t = -1.16$ ,  $p = .66$ ; V2:  $t = -2.07$ ,  $p = .64$ ; V3:  $t = -0.84$ ,  $p = .84$ ; V3A/B:  $t = -0.13$ ,  $p = .90$ ; V4:  $t = -0.15$ ,  $p = .90$ ; IPS0:  $t = -0.26$ ,  $p = .90$ ; IPS1:  $t = 1.19$ ,  $p = .66$ ; IPS2:  $t = 0.29$ ,  $p = .90$ ; LO1:  $t = -0.47$ ,  $p = .90$ ; LO2:  $t = 0.19$ ,  $p = .90$ ; VO1:  $t = 1.28$ ,  $p = .66$ ; Figure 6; two-tailed  $t$  tests, FDR-corrected,

$df = 9$ ), indicating that, for a given cortical area, the amplitude of stimulus-evoked responses does not predict the strength of endogenous fluctuations in that area over the course of a 5-min fMRI run.

Our full data set includes experiments conducted at both a 3T Siemens scanner and a 4T Varian scanner. We therefore separately analyzed data collected at the two scanners. This analysis shows that the correlation between amplitudes at the stimulus and nonstimulus frequencies across runs was significantly greater for participants in the 3T scanner in all topographically organized areas except IPS0, IPS1, LO1, and VO1 (Figure 6; all significant  $p$  values = .04, two-tailed  $t$  tests, FDR-corrected,  $df = 8$ ). However, neither the 3T nor the 4T participant group exhibited values for the correlation between amplitudes at stimulus and nonstimulus frequencies that were significantly different from zero in any topographic area (all  $ps > .05$ ; two-tailed  $t$  tests; FDR-corrected,  $df = 4$ ).

### Visual Target Detection Is Negatively Correlated with Amplitude of Endogenous Fluctuations but not with Amplitude of the Stimulus-Evoked Response

Our results demonstrate that both attentional enhancement of response amplitude and suppression of endogenous fluctuations contributed to improved response reliability in topographic cortical areas. To determine

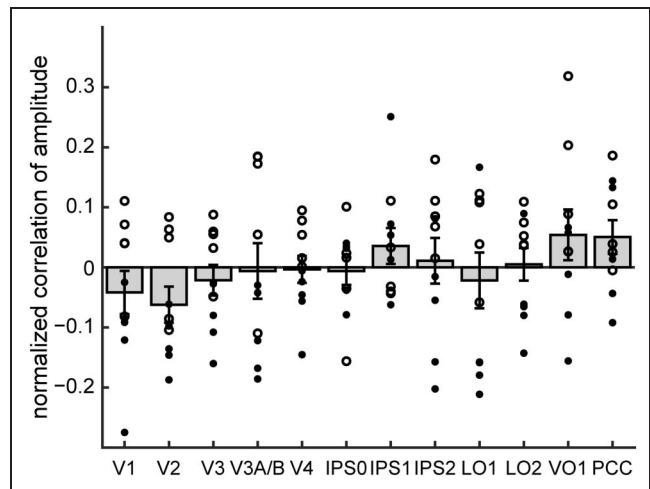


**Figure 6.** Amplitude of stimulus-evoked responses does not correlate with amplitude of slow endogenous fluctuations across 5-min fMRI runs. The amplitude at the stimulus frequency was normalized by subtracting the amplitude of nonstimulus frequency bands on either side of the stimulus frequency band to estimate the strength of the stimulus-evoked response on each attention-to-wedge run. Across runs, this measure of stimulus-evoked response amplitude was not significantly correlated with the magnitude of slow endogenous fluctuations at nonstimulus frequencies in any cortical area. Open circles: individual participant data from 3T scanner; filled circles: individual participant data from 4T scanner. Error bars represent SEMs across participants.

the relative contributions of enhancement and suppression to visual target detection, we correlated the percentage of targets correctly detected in the attention-to-wedge task with fMRI amplitude at both stimulus and nonstimulus frequencies. Each 5-min run generated a single behavioral measure and fMRI measures of the amplitude of both the stimulus-evoked response and endogenous fluctuations at nonstimulus frequencies.

Surprisingly, target detection across attention-to-wedge runs was not correlated with stimulus-evoked response amplitude in any cortical area (V1:  $t = -0.06$ ,  $p = .95$ ; V2:  $t = -0.15$ ,  $p = .95$ ; V3:  $t = -0.18$ ,  $p = .95$ ; V3A/B:  $t = .10$ ,  $p = .95$ ; V4:  $t = .63$ ,  $p = .94$ ; IPS0:  $t = 0.70$ ,  $p = .94$ ; IPS1:  $t = -1.10$ ,  $p = .90$ ; IPS2:  $t = -1.69$ ,  $p = .50$ ; LO1:  $t = -0.80$ ,  $p = .94$ ; LO2:  $t = -2.86$ ,  $p = .23$ ; VO1:  $t = .43$ ,  $p = .95$ ; Figure 7A; two-tailed  $t$  tests, FDR-corrected,  $df = 9$ ). This was also true for the correlation between target detection and the normalized amplitude at the stimulus frequency (V1:  $t = 2.07$ ,  $p = .32$ ; V2:  $t = 1.89$ ,  $p = .32$ ; V3:  $t = 1.52$ ,  $p = .33$ ; V3A/B:  $t = 0.70$ ,  $p = .67$ ; V4:  $t = 1.96$ ,  $p = .32$ ; IPS0:  $t = 1.66$ ,  $p = .32$ ; IPS1:  $t = -0.37$ ,  $p = .86$ ; IPS2:  $t = -0.05$ ,  $p = .96$ ; LO1:  $t = 1.00$ ,  $p = .51$ ; LO2:  $t = -0.13$ ,  $p = .96$ ; VO1:  $t = 1.66$ ,  $p = .32$ ).

Although stronger responses to an attended visual stimulus were not associated with enhanced target detection, we found that this measure of performance across attention-to-wedge runs was significantly negatively correlated with the amplitude of nonstimulus frequencies in all studied topographic areas (V1:  $t = -4.10$ ,  $p = 5.9 \times 10^{-3}$ ; V2:  $t = -5.26$ ,  $p = 5.9 \times 10^{-3}$ ; V3:  $t = -4.22$ ,  $p = 5.9 \times 10^{-3}$ ; V3A/B:  $t = -2.97$ ,  $p = .017$ ; V4:  $t = -3.69$ ,  $p = 7.5 \times 10^{-3}$ ; IPS0:  $t = -4.04$ ,  $p = 5.9 \times 10^{-3}$ ; IPS1:  $t = -2.99$ ,  $p = .017$ ; IPS2:  $t = -3.90$ ,  $p = 6.2 \times 10^{-3}$ ; LO1:  $t = -4.30$ ,  $p = 5.9 \times 10^{-3}$ ; LO2:  $t = -4.77$ ,  $p = 5.9 \times 10^{-3}$ ; VO1:  $t = -3.33$ ,

$p = .012$ ; two-tailed  $t$  tests, FDR-corrected,  $df = 9$ ). Therefore, suppression of slow endogenous fluctuations that were unrelated to the stimulus significantly predicted target detection, as measured behaviorally (Figure 7B).

Correlations of target detection with amplitude at stimulus and nonstimulus frequencies were also computed separately for participants in the 3T and 4T scanners. There were no differences between these two participant groups for either correlation in any of the topographic cortical areas (Figure 7; all  $ps > .05$ , two-tailed  $t$  tests, FDR-corrected,  $df = 8$ ).

We repeated these brain-behavior correlation analyses but used RTs instead of percentage of targets correctly detected. RTs were not significantly correlated with either the amplitude at the stimulus frequency or at nonstimulus frequencies across 5-min runs in any of the topographic cortical areas we studied (all  $ps > .05$ , two-tailed  $t$  tests, FDR-corrected;  $df = 9$ ). However, participants were not under time pressure to respond in the target detection task in our study, and it is possible that correlations between RTs and the fMRI measures we describe in this study would have been evident if the task had emphasized speed of response.

The frequency distribution of the correlation between percentage of targets correctly detected and suppression of slow endogenous fluctuations differed from the frequency distribution of attentional suppression itself. Although suppression of endogenous frequencies was most pronounced at very low frequencies (between 0.0037 Hz, the lowest frequency we could measure, to approximately 0.03 Hz in most areas), the inverse correlation between target detection performance and amplitude of endogenous fluctuations was generally strongest at frequencies above 0.02 Hz and often extended to 0.1 Hz, the highest frequency we analyzed (Figure 8).

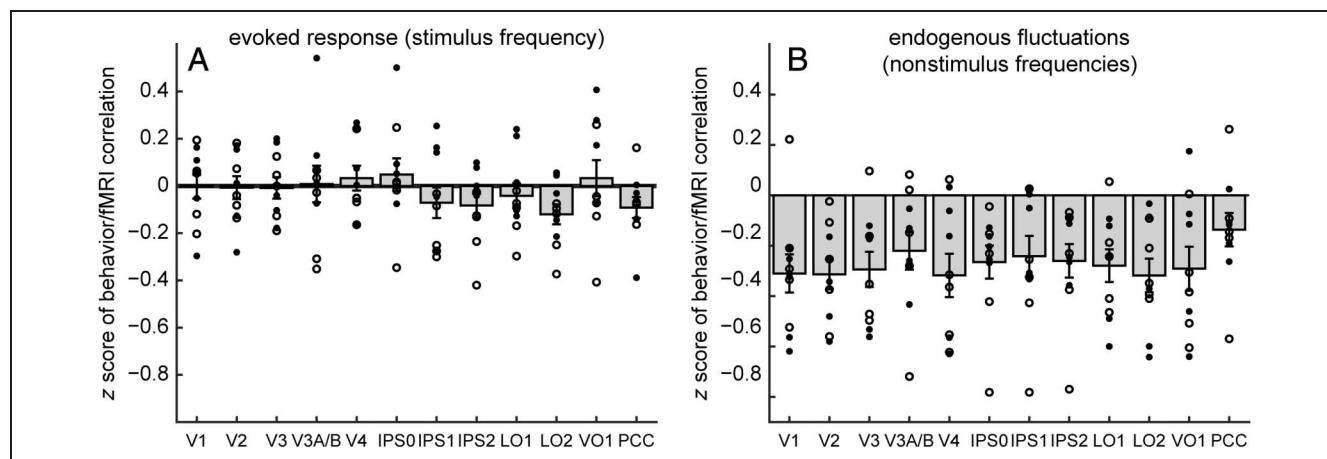


**Figure 7.** Correlation between performance and fMRI amplitude at stimulus and nonstimulus frequencies. (A) Across 5-min runs, no topographically organized area showed a significant correlation between amplitude at the stimulus frequency and the percentage of wedge targets that were correctly detected. (B) Behavioral performance was significantly negatively correlated with amplitude of fMRI fluctuations at nonstimulus frequencies. Open circles: individual participant data from 3T scanner; filled circles: individual participant data from 4T scanner. Error bars represent SEMs across participants.

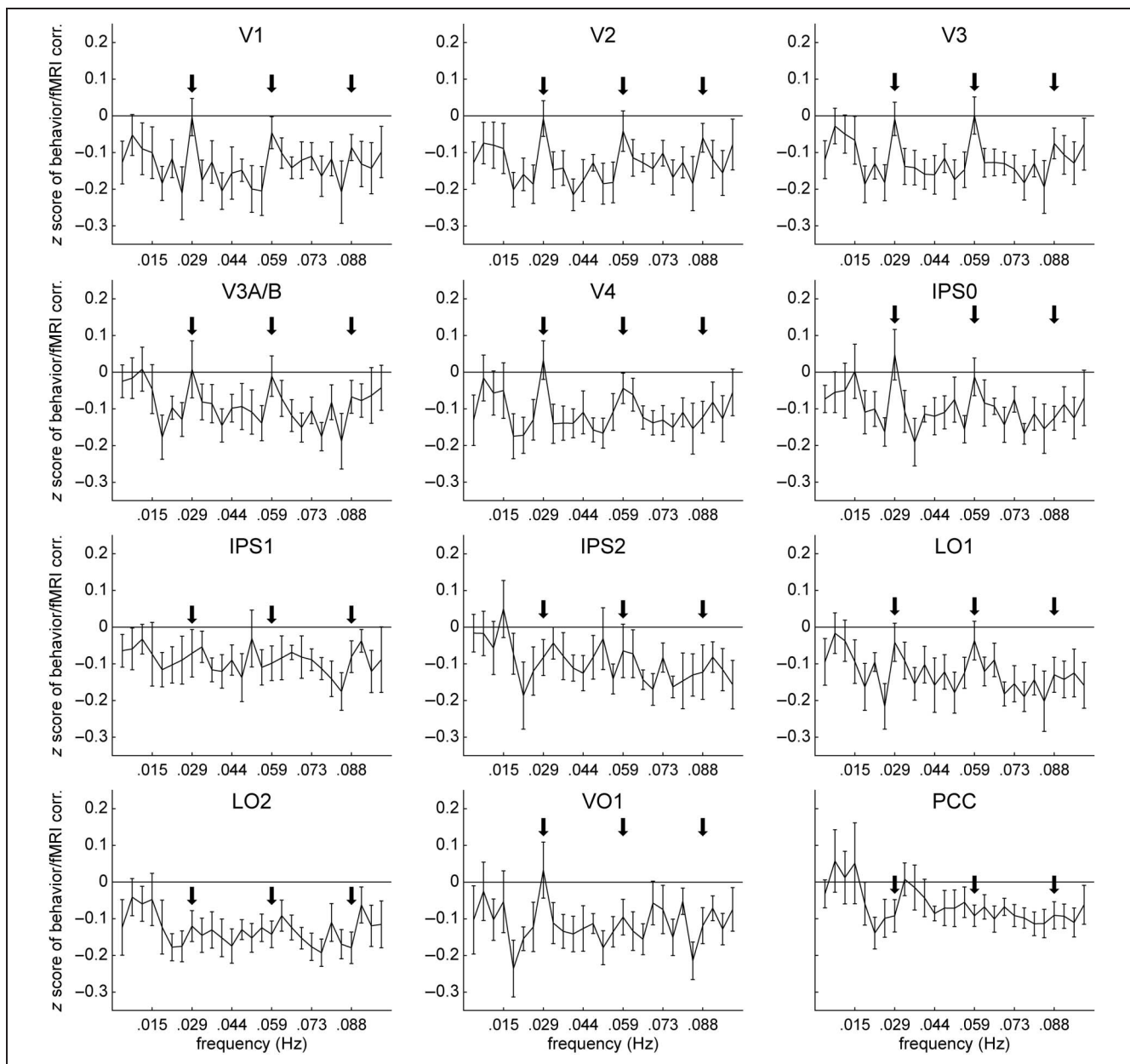


**Figure 8.** Correlation between behavioral performance and amplitude of fluctuations across the frequency spectrum. In all topographically organized areas, negative correlations between performance and endogenous fMRI signal fluctuations tended to be weaker at the slowest nonstimulus frequencies ( $<0.015$  Hz) compared with higher nonstimulus frequencies. Stimulus frequency (0.029 Hz) and associated harmonics (0.059 and 0.088 Hz) are indicated with arrows. Error bars represent *SEMs* across participants.

### Lack of Attentional Effects in a Control Nontopographic PCC Region

The consistent attentional suppression of fMRI activity fluctuations at nonstimulus frequencies across many topographically organized cortical areas raises the possibility of a global effect of allocation of spatial attention to the wedge, relative to attending to the central fixation point. Fluctuations in arterial carbon dioxide concentration (Wise, Ide, Poulin, & Tracey, 2004), cardiac rate (Shmueli et al., 2007), and respiratory rate (Birn, Diamond, Smith, & Bandettini, 2006) occur within the 0.0037–0.1 Hz range that we used to measure fMRI

fluctuations in nonstimulus frequencies, and these non-neural fluctuations likely influenced our measured BOLD signals. Additionally, although we matched task difficulty in the attention-to-fixation and attention-to-wedge conditions for every participant in our study, it is still possible that allocating covert spatial attention to the wedge resulted in a global reduction in the amplitude of endogenous BOLD fluctuations in nontopographic brain regions.

To control for this possibility, we anatomically defined an ROI in the PCC/precuneus (Greicius et al., 2003) of each participant (see the Methods section). The PCC/precuneus is part of a network of regions that

exhibits reduced activity during attention-demanding cognitive processing (Greicius et al., 2003) and spontaneous activity that is negatively correlated with activity in visual cortical regions (Fransson, 2006; Fox et al., 2005). Relative to the attention-to-fixation condition, attending to the wedge did not have a significant effect on either the amplitude of the stimulus-evoked response ( $t = -0.70, p = .53$ ; Figure 3A) or endogenous fluctuations at nonstimulus frequencies ( $t = -0.63, p = .53$ ; Figure 3B) in the PCC/precuneus (two-tailed  $t$  tests, FDR-corrected,  $df = 59$ ; see also Figures 4 and 5). Moreover, attentional enhancement of the stimulus-evoked response was significantly greater in all topographic regions (V1:  $t = 5.93, p = 3.7 \times 10^{-7}$ ; V2:  $t = 5.98, p = 3.7 \times 10^{-7}$ ; V3:  $t = 6.06, p = 3.7 \times 10^{-7}$ ; V3A/B:  $t = 4.17, p = 1.9 \times 10^{-4}$ ; V4:  $t = 8.22, p = 2.6 \times 10^{-10}$ ; IPS0:  $t = 3.16, p = 3.9 \times 10^{-3}$ ; IPS1:  $t = 2.25, p = .034$ ; IPS2:  $t = 2.28, p = .034$ ; VO1:  $t = 7.83, p = 5.9 \times 10^{-10}$ ) except LO1 and LO2 (LO1:  $t = 1.12, p = .27$ ; LO2:  $t = 1.88, p = .071$ ) than in PCC/precuneus (two-tailed paired  $t$  tests, FDR-corrected for 11 statistical tests,  $df = 59$ ), and attentional suppression at nonstimulus frequencies was significantly greater in all topographic regions (V1:  $t = -2.52, p = .020$ ; V2:  $t = -2.70, p = .014$ ; V3:  $t = -3.05, p = 6.2 \times 10^{-3}$ ; V3A/B:  $t = -4.07, p = 1.5 \times 10^{-3}$ ; IPS0:  $t = -3.81, p = 1.8 \times 10^{-3}$ ; IPS1:  $t = -3.60, p = 1.8 \times 10^{-3}$ ; LO1:  $t = -3.36, p = 3.0 \times 10^{-3}$ ; LO2:  $t = -3.62, p = 1.8 \times 10^{-3}$ ) except V4, IPS2, and VO1 (V4:  $t = -1.60, p = .13$ ; IPS2:  $t = -1.88, p = .079$ ; VO1:  $t = -1.27, p = .21$ ) than in PCC/precuneus (two-tailed paired  $t$  tests, FDR-corrected,  $df = 59$ ).

In addition, there was not a significant correlation between behavioral performance in attend-to-wedge runs and either response amplitude ( $t = -2.08, p = .040$ ; Figure 7A) or amplitude at nonstimulus frequencies ( $t = -2.05, p = .070$ ; Figure 7B) in the PCC/precuneus (two-tailed  $t$  tests, FDR-corrected,  $df = 9$ ; see also Figure 8). However, direct statistical comparisons of PCC/precuneus correlation values with those of individual topographically organized areas revealed no significant differences for raw stimulus frequency (V1:  $t = 1.17, p = .50$ ; V2:  $t = 1.18, p = .50$ ; V3:  $t = 1.20, p = .50$ ; V3A/B:  $t = 1.05, p = .51$ ; V4:  $t = 1.89, p = .50$ ; IPS0:  $t = 1.50, p = .50$ ; IPS1:  $t = 0.23, p = .90$ ; IPS2:  $t = 0.13, p = .90$ ; LO1:  $t = 0.65, p = .73$ ; LO2:  $t = -0.40, p = .85$ ; VO1:  $t = 1.41, p = .50$ ), normalized stimulus frequency (V1:  $t = 2.07, p = .21$ ; V2:  $t = 1.90, p = .21$ ; V3:  $t = 1.65, p = .24$ ; V3A/B:  $t = 1.03, p = .45$ ; V4:  $t = 2.06, p = .21$ ; IPS0:  $t = 1.94, p = .21$ ; IPS1:  $t = 0.29, p = .78$ ; IPS2:  $t = 0.55, p = .67$ ; LO1:  $t = 1.17, p = .43$ ; LO2:  $t = 0.53, p = .67$ ; VO1:  $t = 1.87, p = .21$ ), or nonstimulus frequencies (V1:  $t = -1.94, p = .28$ ; V2:  $t = -2.16, p = .28$ ; V3:  $t = -1.62, p = .28$ ; V3A/B:  $t = -0.73, p = .48$ ; V4:  $t = -1.85, p = .28$ ; IPS0:  $t = -1.08, p = .39$ ; IPS1:  $t = -0.78, p = .48$ ; IPS2:  $t = -1.05, p = .39$ ; LO1:  $t = -1.47, p = .28$ ; LO2:  $t = -1.71, p = .28$ ; VO1:  $t = -1.45, p = .28$ ; paired two-tailed  $t$  tests, FDR-corrected,  $df = 9$ ).

## DISCUSSION

Allocation of spatial attention to a visual stimulus improves the reliability of the BOLD response to that stimulus (Bressler & Silver, 2010). In this study, we show that this increase in reliability is partly due to a reduction in the strength of slow endogenous fluctuations that are unrelated to the visual stimulus. This attentional suppression of endogenous activity was observed in every topographic cortical area we studied except IPS2, V4 and VO1. An increase in the amplitude of the stimulus-evoked response when attending the wedge also contributed to increased response reliability in early and ventral visual cortical areas. However, although the magnitude of the stimulus-evoked response was not predictive of participants' ability to detect targets within the wedge across 5-min runs, suppression of slow endogenous fluctuations was highly correlated with successful target detection in all studied topographic areas.

### Attentional Enhancement of Stimulus-Evoked Responses

We found that allocating spatial attention to the rotating wedge stimulus enhanced the BOLD response evoked by the wedge. This enhancement was strongest in ventral areas V4 and VO1; moderate in early visual areas V1, V2, and V3; small but significant in dorsal areas V3A/B and IPS0; and not significant in posterior parietal cortical areas IPS1/2 and lateral occipital areas LO1/2. The lack of attentional modulation of the stimulus-evoked response in IPS areas is consistent with that reported in Corbetta, Kincade, Ollinger, McAvoy, and Shulman (2000) and does not necessarily contradict previous studies showing robust attentional modulation of BOLD activity in this region (Silver et al., 2005; Yantis et al., 2002), as these studies did not directly compare IPS responses to attended and unattended visual stimuli.

Additionally, we found no attentional enhancement of the stimulus-evoked response in LO1/2, consistent with a previous study showing a similar lack of attentional enhancement of LO visual responses for stimuli with greater than 30% contrast (Murray & He, 2006). However, we previously reported robust attentional enhancement of fMRI responses in LO1/2 (Bressler, Fortenbaugh, Robertson, & Silver, 2013). There are multiple differences in experimental design and attentional demands between that study and this study, including the spatial extent of the attended region (much larger in this study), continuous attentional tracking of a moving stimulus versus discrete shifts of attention to an unpredictable location in Bressler et al. (2013), and the presence of distractors in Bressler et al. (2013). Further research is needed to determine the relative contribution of these various factors to modulation of LO1/2 responses by spatial attention.

## **Attentional Suppression of Slow Endogenous Fluctuations**

We found attentional suppression of slow (<0.1 Hz) endogenous fluctuations in every topographic cortical area we studied except IPS2, V4, and VO1. We matched the visual stimulus and task difficulty in the two attention conditions, allowing us to attribute changes in the magnitude of slow fluctuations to changes in spatial attention. Moreover, our task and stimulus design are uniquely suited to reveal effects of attention at very slow frequencies of fluctuations in brain activity that are unrelated to stimulus-evoked responses. On alternate 5-min runs, attention was directed either to a central fixation point or to a peripheral visual stimulus that was rotating at 0.03 Hz. Fourier analysis of the fMRI response therefore distinguishes between effects of attention on amplitude at the stimulus frequency from effects on amplitude of endogenous fluctuations in fMRI signals at other frequencies. Most fMRI studies of spatial attention employ either event-related or block designs in trial-based paradigms to assess the effects of discrete shifts of spatial attention. In these designs, the experimental effects are typically not constrained to specific frequency bands, and they are usually not compatible with measuring effects of attention on slow fluctuations in brain activity (Huk, Bonnen, & He, 2018). Therefore, our design enables us to assess effects that would be very difficult to discover using more standard visual attention paradigms.

## **Relationships among Slow fMRI Fluctuations, Neural Activity, and Behavior**

Fluctuations in fMRI signal in the frequency range that we have studied (<0.1 Hz) are likely to be influenced by both neural and nonneural factors. For example, fluctuations in arterial carbon dioxide concentration (Wise et al., 2004), cardiac rate (Shmueli et al., 2007), and respiratory rate (Birn et al., 2006) all occur at these frequencies. For this reason, many studies apply a high-pass filter during preprocessing of the fMRI BOLD response to reduce the contributions of these sources of “noise.” However, neural activity also contributes to slow endogenous fluctuations in fMRI signals. The amplitude of BOLD responses to a given stimulus is correlated with levels of single-unit spiking, multiunit activity, and local field potential gamma power (Mukamel et al., 2005; Logothetis, Pauls, Augath, Trinath, & Oeltermann, 2001), and similar relationships between fMRI signals and direct measures of neuronal activity have also been observed for slow endogenous fluctuations (Keller et al., 2013; Schölvinck, Maier, Ye, Duyn, & Leopold, 2010; Shmuel & Leopold, 2008). Therefore, the BOLD signals in the very slow range that we have studied (<0.1 Hz) likely include components that reflect neural activity.

Moreover, fluctuations in brain activity on this time-scale are cognitively and behaviorally relevant. The global

component of resting state fMRI measurements has been associated with general levels of arousal and alertness (Turchi et al., 2018; Wong, Olafsson, Tal, & Liu, 2013). Within the frequency range we have studied (<0.1 Hz), stimulus detection is predicted by spontaneous slow negative cortical shifts in EEG signals (Devrim, Demiralp, Kurt, & Yücesir, 1999) and by the phase of ongoing EEG oscillations in the infraslow range (Monto et al., 2008). Additionally, previous studies have demonstrated relationships between performance on visual detection tasks and prestimulus fMRI activity recorded a few seconds before stimulus onset (Coste & Kleinschmidt, 2016; Wohlschläger et al., 2016; Schölvinck, Friston, & Rees, 2012; Hesselmann et al., 2008), and fMRI connectivity between brain regions at very slow frequencies is significantly correlated with performance across participants in an executive control task (Xu et al., 2014) and a visual attention task (Griffis, Elkhatali, Burge, Chen, & Visscher, 2015). Our results extend these findings by showing that spatial attention suppresses slow endogenous fluctuations in occipital and parietal cortex and that reduced endogenous activity predicts performance on a visual detection task.

Various theories have been proposed regarding the roles of slow endogenous activity fluctuations in cortical function, including self-regulation of cortical excitability to avoid overactivation and insensitivity (Birbaumer, Elbert, Canavan, & Rockstroh, 1990), generation of predictive internal models of the environment (Berkes, Orbán, Lengyel, & Fiser, 2011), providing a substrate for top-down expectation signals (Ringach, 2009), and integrating information across wide regions of cortex to support consciousness (He & Raichle, 2009). One additional possibility is that slow endogenous fluctuations are important for coordinating neural activity across distant regions of cortex in the service of nonperceptual functions but that they can also divert resources from performance of specific perceptual tasks and/or interfere with representations of sensory information.

## **Differential Amounts of Attentional Enhancement of Stimulus-Evoked Responses and Attentional Suppression of Endogenous Fluctuations across Cortical Areas**

We found that the relative amounts of attentional enhancement of the visually evoked response and suppression of endogenous fluctuations varied across areas. In early and ventral visual cortical areas, an increase in the strength of the evoked response contributed to enhanced response reliability, but this effect was not observed in posterior parietal cortical areas IPS1 and IPS2 or in lateral occipital cortical areas. In contrast, every topographic cortical area we studied, except IPS2, V4 and VO1, exhibited a significant decrease in endogenous fluctuations at nonstimulus frequencies that also contributed to enhanced response reliability.

Ventral cortical areas V4 and VO1 exhibited the strongest increases in stimulus-evoked response and the weakest reductions in the strength of ongoing fluctuations. In contrast, dorsal areas V3A/B, IPS0, and IPS1, as well as lateral occipital areas LO1 and LO2, showed little or no increase in evoked response and the strongest reductions in endogenous fluctuations. Early visual cortical areas V1–V3 displayed intermediate levels of both response enhancement and suppression at nonstimulus frequencies by attention.

### **Effects of Attention on Enhancement, Suppression, and Response Reliability**

Although our results reveal an inverse relationship between the amount of attentional enhancement of the response to the stimulus and attentional suppression of endogenous fluctuations across cortical areas, these two effects are unrelated across fMRI runs within a cortical area. That is, the amplitude of the stimulus-evoked response and the amplitude of slow endogenous fluctuations of nonstimulus frequencies were not significantly correlated, suggesting that they may reflect dissociable mechanisms, at least at the timescale studied here (5-min runs). Previous studies have also shown dissociations between effects of attention on evoked responses and on correlated activity fluctuations in pairs of neurons in macaque visual cortex (Ruff & Cohen, 2014; Herrero et al., 2013).

Studies employing microelectrode recordings have revealed that spatial attention enhances response reliability, both by increasing the evoked response amplitude (McAdams & Maunsell, 1999) and by decreasing intertrial response variability (Cohen & Maunsell, 2009; Mitchell et al., 2007, 2009). Attention can also enhance response reliability by decorrelating fluctuations in spiking within neuronal populations (Ruff & Cohen, 2014; Herrero et al., 2013; Cohen & Maunsell, 2009; Mitchell et al., 2009). These studies describe attentional suppression of correlated activity on much shorter timescales than those for which we have demonstrated attentional suppression of endogenous fluctuations of fMRI signals. However, the strength of local interneuronal correlations is itself correlated with BOLD activity (Nir et al., 2007).

Attentional enhancement of the stimulus-evoked response was significantly greater in all topographically defined regions (except LO1 and LO2) than in a control nontopographic cortical region (PCC/precuneus). In addition, attentional suppression of endogenous fluctuations was significantly greater in all topographically defined regions (except V4, IPS2, and VO1) than in PCC/precuneus. However, the distinction between topographic areas and this control area was less clear for correlations between behavior and strength of endogenous fluctuations: Although all topographic regions exhibited a significant correlation and the control PCC/precuneus region did not, there were no significant differences in

correlation coefficients between individual topographic regions and PCC/precuneus.

These results suggest that the negative correlation between behavioral performance on the attention-to-wedge task and the strength of slow endogenous fluctuations (Figure 7B) may be more widespread across cortical areas than the effects of attending to the wedge (as compared with attending to fixation) on the amplitude of slow endogenous fluctuations (Figure 3B). In addition, attentional suppression of endogenous fluctuations was strongest at very low temporal frequencies (<0.03 Hz; Figure 4), whereas the negative correlation between target detection performance and the amplitude of endogenous fluctuations was more evident at higher temporal frequencies (>0.02 Hz; Figure 8).

### **Conclusions**

In addition to increasing the strength of visually evoked BOLD responses, sustained covert visual spatial attention to a periodic stimulus decreased the strength of endogenous BOLD fluctuations. Reduced endogenous activity substantially contributed to improved response reliability in every topographically organized cortical area we studied except IPS2, V4, and VO1 and was inversely correlated with behavioral performance in all topographic areas. In contrast, attention's effects on visually evoked BOLD responses contributed to improved response reliability only in early and ventral cortical areas, and the amplitude of stimulus-evoked responses did not predict behavioral performance in any area. Therefore, our results provide evidence that attentional suppression of endogenous fluctuations in brain activity enhances cortical representations of visual stimuli and substantially benefits visual perception.

### **Acknowledgments**

This work was supported by the National Eye Institute at the National Institutes of Health (R01 EY025278 to M. A. S., Training Grant in Vision Science T32 EY07043, and Core Grant for Vision Research P30 EY003176), the National Science Foundation (Graduate Research Fellowship to D. W. B. and Major Instrumentation Program grant BCS-0821855), and the National Institute on Aging at the National Institutes of Health (NRSA F31 AG032209 to A. R.).

Reprint requests should be sent to Michael Silver, School of Optometry, 360 Minor Hall, University of California, Berkeley, Berkeley, CA 94720-2020, or via e-mail: masilver@berkeley.edu.

### **REFERENCES**

- Berkes, P., Orbán, G., Lengyel, M., & Fiser, J. (2011). Spontaneous cortical activity reveals hallmarks of an optimal internal model of the environment. *Science*, *331*, 83–87.
- Birbaumer, N., Elbert, T., Canavan, A. G., & Rockstroh, B. (1990). Slow potentials of the cerebral cortex and behavior. *Physiological Review*, *70*, 1–41.

- Birn, R. M., Diamond, J. B., Smith, M. A., & Bandettini, P. A. (2006). Separating respiratory-variation-related fluctuations from neuronal-activity-related fluctuations in fMRI. *Neuroimage*, *31*, 1536–1548.
- Bressler, D. W., Fortenbaugh, F. C., Robertson, L. C., & Silver, M. A. (2013). Visual spatial attention enhances the amplitude of positive and negative fMRI responses to visual stimulation in an eccentricity-dependent manner. *Vision Research*, *85*, 104–112.
- Bressler, D. W., & Silver, M. A. (2010). Spatial attention improves reliability of fMRI retinotopic mapping signals in occipital and parietal cortex. *Neuroimage*, *53*, 526–533.
- Brewer, A. A., Liu, J., Wade, A. R., & Wandell, B. A. (2005). Visual field maps and stimulus selectivity in human ventral occipital cortex. *Nature Neuroscience*, *8*, 1102–1109.
- Busch, N. A., Dubois, J., & VanRullen, R. (2009). The phase of ongoing EEG oscillations predicts visual perception. *Journal of Neuroscience*, *29*, 7869–7876.
- Carrasco, M. (2011). Visual attention: The past 25 years. *Vision Research*, *51*, 1484–1525.
- Cohen, M. R., & Maunsell, J. H. R. (2009). Attention improves performance primarily by reducing interneuronal correlations. *Nature Neuroscience*, *12*, 1594–1600.
- Corbetta, M., Kincade, J. M., Ollinger, J. M., McAvoy, M. P., & Shulman, G. L. (2000). Voluntary orienting is dissociated from target detection in human posterior parietal cortex. *Nature Neuroscience*, *3*, 292–297.
- Coste, C. P., & Kleinschmidt, A. (2016). Cingulo-opercular network activity maintains alertness. *Neuroimage*, *128*, 264–272.
- Devrim, M., Demiralp, T., Kurt, A., & Yücesir, I. (1999). Slow cortical potential shifts modulate the sensory threshold in human visual system. *Neuroscience Letters*, *270*, 17–20.
- Engel, S. A., Rumelhart, D. E., Wandell, B. A., Lee, A. T., Glover, G. H., Chichilnisky, E. J., et al. (1994). fMRI of human visual cortex. *Nature*, *369*, 525.
- Fox, M. D., Snyder, A. Z., Vincent, J. L., Corbetta, M., Van Essen, D. C., & Raichle, M. E. (2005). The human brain is intrinsically organized into dynamic, anticorrelated functional networks. *Proceedings of the National Academy of Sciences, U.S.A.*, *102*, 9673–9678.
- Fransson, P. (2006). How default is the default mode of brain function? Further evidence from intrinsic BOLD signal fluctuations. *Neuropsychologia*, *44*, 2836–2845.
- Gandhi, S. P., Heeger, D. J., & Boynton, G. M. (1999). Spatial attention affects brain activity in human primary visual cortex. *Proceedings of the National Academy of Sciences, U.S.A.*, *96*, 3314–3319.
- Genovese, C. R., Lazar, N. A., & Nichols, T. (2002). Thresholding of statistical maps in functional neuroimaging using the false discovery rate. *Neuroimage*, *15*, 870–878.
- Greicius, M. D., Krasnow, B., Reiss, A. L., & Menon, V. (2003). Functional connectivity in the resting brain: A network analysis of the default mode hypothesis. *Proceedings of the National Academy of Sciences, U.S.A.*, *100*, 253–258.
- Griffis, J. C., Elkhetafi, A. S., Burge, W. K., Chen, R. H., & Visscher, K. M. (2015). Retinotopic patterns of background connectivity between V1 and fronto-parietal cortex are modulated by task demands. *Frontiers in Human Neuroscience*, *9*, 338.
- He, B. J., & Raichle, M. E. (2009). The fMRI signal, slow cortical potential and consciousness. *Trends in Cognitive Sciences*, *13*, 302–309.
- Herrero, J. L., Gieselmann, M. A., Sanayei, M., & Thiele, A. (2013). Attention-induced variance and noise correlation reduction in macaque V1 is mediated by NMDA receptors. *Neuron*, *78*, 729–739.
- Hesselmann, G., Kell, C. A., & Kleinschmidt, A. (2008). Ongoing activity fluctuations in hMT+ bias the perception of coherent visual motion. *Journal of Neuroscience*, *28*, 14481–14485.
- Huk, A., Bonnen, K., & He, B. J. (2018). Beyond trial-based paradigms: Continuous behavior, ongoing neural activity, and natural stimuli. *Journal of Neuroscience*, *38*, 7551–7558.
- Imamoglu, F., Heinzle, J., Imfeld, A., & Haynes, J. D. (2014). Activity in high-level brain regions reflects visibility of low-level stimuli. *Neuroimage*, *102*, 688–694.
- Jenkinson, M., Bannister, P., Brady, M., & Smith, S. (2002). Improved optimization for the robust and accurate linear registration and motion correction of brain images. *Neuroimage*, *17*, 825–841.
- Keller, C. J., Bickel, S., Honey, C. J., Groppe, D. M., Entz, L., Craddock, R. C., et al. (2013). Neurophysiological investigation of spontaneous correlated and anticorrelated fluctuations of the BOLD signal. *Journal of Neuroscience*, *33*, 6333–6342.
- Larsson, J., & Heeger, D. J. (2006). Two retinotopic visual areas in human lateral occipital cortex. *Journal of Neuroscience*, *26*, 13128–13142.
- Logothetis, N. K., Pauls, J., Augath, M., Trinath, T., & Oeltermann, A. (2001). Neurophysiological investigation of the basis of the fMRI signal. *Nature*, *412*, 150–157.
- Mathewson, K. E., Gratton, G., Fabiani, M., Beck, D. M., & Ro, T. (2009). To see or not to see: Prestimulus alpha phase predicts visual awareness. *Journal of Neuroscience*, *29*, 2725–2732.
- Maunsell, J. H. R. (2015). Neuronal mechanisms of visual attention. *Annual Review of Vision Science*, *1*, 373–391.
- McAdams, C. J., & Maunsell, J. H. R. (1999). Effects of attention on the reliability of individual neurons in monkey visual cortex. *Neuron*, *23*, 765–773.
- Mitchell, J. F., Sundberg, K. A., & Reynolds, J. H. (2007). Differential attention-dependent response modulation across cell classes in macaque visual area V4. *Neuron*, *55*, 131–141.
- Mitchell, J. F., Sundberg, K. A., & Reynolds, J. H. (2009). Spatial attention decorrelates intrinsic activity fluctuations in macaque area V4. *Neuron*, *63*, 879–888.
- Monto, S., Palva, S., Voipio, J., & Palva, J. M. (2008). Very slow EEG fluctuations predict the dynamics of stimulus detection and oscillation amplitudes in humans. *Journal of Neuroscience*, *28*, 8268–8272.
- Mukamel, R., Gelbard, H., Arieli, A., Hasson, U., Fried, I., & Malach, R. (2005). Coupling between neuronal firing, field potentials, and fMRI in human auditory cortex. *Science*, *309*, 951–954.
- Müller, N. G., & Kleinschmidt, A. (2004). The attentional ‘spotlight’s penumbra: Center-surround modulation in striate cortex. *NeuroReport*, *15*, 977–980.
- Murray, S. O., & He, S. (2006). Contrast invariance in the human lateral occipital complex depends on attention. *Current Biology*, *16*, 606–611.
- Nir, Y., Fisch, L., Mukamel, R., Gelbard-Sagiv, H., Arieli, A., Fried, I., et al. (2007). Coupling between neuronal firing rate, gamma LFP, and BOLD fMRI is related to interneuronal correlations. *Current Biology*, *17*, 1275–1285.
- Ress, D., Backus, B. T., & Heeger, D. J. (2000). Activity in primary visual cortex predicts performance in a visual detection task. *Nature Neuroscience*, *3*, 940–945.
- Ringach, D. L. (2009). Spontaneous and driven cortical activity: Implications for computation. *Current Opinion in Neurobiology*, *19*, 439–444.
- Ruff, D. A., & Cohen, M. R. (2014). Attention can either increase or decrease spike count correlations in visual cortex. *Nature Neuroscience*, *17*, 1591–1597.
- Schölvinck, M. L., Friston, K. J., & Rees, G. (2012). The influence of spontaneous activity on stimulus processing in primary visual cortex. *Neuroimage*, *59*, 2700–2708.
- Schölvinck, M. L., Maier, A., Ye, F. Q., Duyn, J. H., & Leopold, D. A. (2010). Neural basis of global resting-state fMRI activity.

- Proceedings of the National Academy of Sciences, U.S.A.*, 107, 10238–10243.
- Sereno, M. I., Dale, A. M., Reppas, J. B., Kwong, K. K., Belliveau, J. W., Brady, T. J., et al. (1995). Borders of multiple visual areas in humans revealed by functional magnetic resonance imaging. *Science*, 268, 889–893.
- Shmuel, A., & Leopold, D. A. (2008). Neuronal correlates of spontaneous fluctuations in fMRI signals in monkey visual cortex: Implications for functional connectivity at rest. *Human Brain Mapping*, 29, 751–761.
- Shmueli, K., van Gelderen, P., de Zwart, J. A., Horowitz, S. G., Fukunaga, M., Jansma, J. M., et al. (2007). Low-frequency fluctuations in the cardiac rate as a source of variance in the resting-state fMRI BOLD signal. *Neuroimage*, 38, 306–320.
- Silver, M. A., Ress, D., & Heeger, D. J. (2005). Topographic maps of visual spatial attention in human parietal cortex. *Journal of Neurophysiology*, 94, 1358–1371.
- Silver, M. A., Ress, D., & Heeger, D. J. (2007). Neural correlates of sustained spatial attention in human early visual cortex. *Journal of Neurophysiology*, 97, 229–237.
- Supèr, H., van der Togt, C., Spekreijse, H., & Lamme, V. A. F. (2003). Internal state of monkey primary visual cortex (V1) predicts figure-ground perception. *Journal of Neuroscience*, 23, 3407–3414.
- Turchi, J., Chang, C., Ye, F. Q., Russ, B. E., Yu, D. K., Cortes, C. R., et al. (2018). The basal forebrain regulates global resting-state fMRI fluctuations. *Neuron*, 97, 940–952.
- Wandell, B. A., Chial, S., & Backus, B. T. (2000). Visualization and measurement of the cortical surface. *Journal of Cognitive Neuroscience*, 12, 739–752.
- Weissman, D. H., Roberts, K. C., Visscher, K. M., & Woldorff, M. G. (2006). The neural bases of momentary lapses in attention. *Nature Neuroscience*, 9, 971–978.
- Wise, R. G., Ide, K., Poulin, M. J., & Tracey, I. (2004). Resting fluctuations in arterial carbon dioxide induce significant low frequency variations in BOLD signal. *Neuroimage*, 21, 1652–1664.
- Wohlschläger, A. M., Glim, S., Shao, J., Draheim, J., Köhler, L., Lourenço, S., et al. (2016). Ongoing slow fluctuations in V1 impact on visual perception. *Frontiers in Human Neuroscience*, 10, 411.
- Wong, C. W., Olafsson, V., Tal, O., & Liu, T. T. (2013). The amplitude of the resting-state fMRI global signal is related to EEG vigilance measures. *Neuroimage*, 83, 983–990.
- Xu, J., Rees, G., Yin, X., Song, C., Han, Y., Ge, H., et al. (2014). Spontaneous neuronal activity predicts intersubject variations in executive control of attention. *Neuroscience*, 263, 181–192.
- Yantis, S., Schwarzbach, J., Serences, J. T., Carlson, R. L., Steinmetz, M. A., Pekar, J. J., et al. (2002). Transient neural activity in human parietal cortex during spatial attention shifts. *Nature Neuroscience*, 5, 995–1002.
- Zarahn, E., Aguirre, G. K., & D’Esposito, M. (1997). Empirical analyses of BOLD fMRI statistics. I. Spatially unsmoothed data collected under null-hypothesis conditions. *Neuroimage*, 5, 179–197.